COMPARISON OF GONG AND MDI SOUND-SPEED ANOMALIES BENEATH TWO ACTIVE REGIONS

S.J. Hughes[1], S.P. Rajaguru[2], and M.J. Thompson[1]

[1]Space & Atmospheric Physics Group, The Blackett Laboratory, Imperial College, London, SW7 2AZ, UK, Email: stephen.hughes1@imperial.ac.uk

[2]Indian Institute of Astrophysics, Koramangala,Bangalore 560 034, India

ABSTRACT

Travel times of acoustic waves are calculated from Dopplergrams of solar oscillations obtained using the Global Oscillation Network Group (GONG) ground-based network and the Michelson Doppler Imager (MDI) instrument on board the SOHO satellite. These travel times are inverted using a standard ray approximation to ascertain the sound-speed anomalies below two active regions. Some simple methods for ignoring the possibly corrupted measurements from within a sunspot are considered, as are diagnostics for optimizing the inversion. Results are then presented for two different spot regions and the results of the instruments are compared: both regions behave in similar ways and the agreement between the two instruments is good. First-skip and second-skip data are found to produce similar results for deeper layers of the model, but the significance of the shallower results from second-skip data is questionable. We conclude that the use of GONG data for time-distance analysis is appropriate

Key words: Sun: activity; Sun: oscillations; sunspots.

1. INTRODUCTION

The recent improvements to the Global Oscillations Network Group (GONG) system for solar oscillations detection has increased the resolution of the photospheric Doppler velocities to a level comparable with that of the full-disk mode of the Michelson Doppler Imager (MDI) instrument aboard the Solar and Heliospheric Observatory (SOHO). It is important to make comparisons between the two instruments, and to identify any differences in inferred properties of the sub-surface layers.

This work focuses on the estimation of sound-speed anomalies in the near-surface layers of the convection zone in order to compare the data from the MDI and GONG instruments. Horizontal inhomogeneities in the propagation speed of sound waves in the near-surface region can result from variations in temperature associated with convective structures and from the presence of a magnetic field, for instance directly underneath a sunspot. Information about such acoustic inhomogeneities is revealing about subsurface conditions. We use the techniques of time-distance helioseismology to infer the properties of such inhomogeneities from observations of the solar surface.

2. ANALYSIS METHOD

Time-distance helioseismology (Duvall et al., 1993) attempts to make measurements of parameters that affect wave propagation in the convection zone, specifically via the recovery of wave travel-times, by comparing measured properties of oscillations at the surface.

Ray-based kernels that represent the forward model for the waves were computed for the purpose of measuring sound-speed anomalies after Giles (2000). The travel-time data were computed on a regular grid of 20×20 values with a centre-annulus geometry. The grid cells correspond to the pixels of the relevant instrument such that the data forms a map that spans 28.4 Mm in the case of MDI and 34.6 Mm for GONG, in each of the horizontal dimensions. We combine several of these maps to improve the spatial coverage.

The inversions use the LSQR algorithm of Paige and Saunders (1982), an iterative scheme in which larger-scale, smoother components of the solution tend to converge first. In order to make the inversion more effective we have made some choices about the parametrization of our model. The depth spacing of grid is in constant acoustic depth, although when displaying results we interpolate back to a regular depth spacing. The horizontal grid spacings are chosen to maximize the resolution in the central region that corresponds to the location of the annular centre-points. To obtain a solution on a larger spatial scale, inversions of nine overlapping travel-time maps that scan over the spot are then combined in a weighted average.

Spots are areas of significant perturbation and we have considered some simple strategies to avoid using direct measurements within the umbra. One technique is to not use those measurements from within the spot itself, an

Proceedings of the SOHO 14 / GONG 2004 Workshop, New Haven, Connecticut, USA, 12-16 July 2004
(ESA SP-559, October 2004)

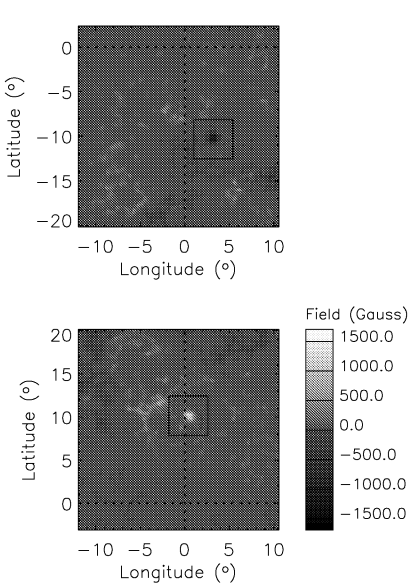

Figure 1. Magnetograms for April 11$^{\rm th}$ (top panel) and April 13$^{\rm th}$ (bottom panel) from MDI. The spatial scale of each analysed region is indicated by the small box. These images show the locations of the spot regions relative to the central meridian and solar equator (dotted lines).

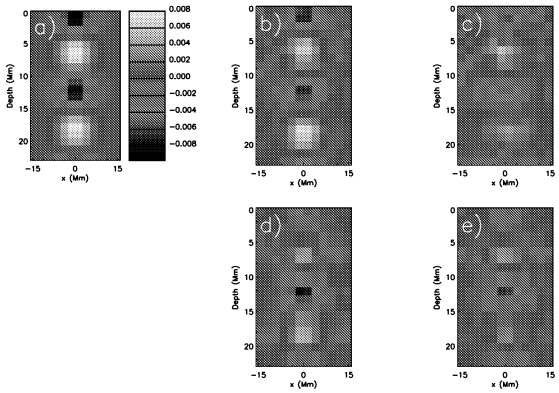

Figure 2. Synthetic sound-speed perturbation model and inversion results. The images are vertical slices, with depth increasing down the page. The colour scale is identical for each panel. The original model is in the upper-left panel (a), the results of inverting first-skip artificial data are shown in the left- (b) and right-hand (c) panels of the same row, while corresponding results from second-skip artificial data are shown in the lower row for cropped (d) and uncropped (e). The results in the right-hand column are from using data cropped to exclude measurements taken directly above the region of non-zero sound-speed perturbation. This represents a best-case scenario, as we have added no noise to the modelled travel times.

approach has been used before by Zhao and Kosovichev (2003) for investigating material flows around sunspots. Practically, this takes the form of ignoring the travel-time data from those centre-annulus cross-correlations for which the centre lies within the spot region. We refer to removing such data as 'cropping' the travel-time maps.

Another approach is to use travel-time maps computed from the measurements of the second skip of the wave-packet: a technique previously considered by Duvall (1995) and Braun et al. (1997). The spatial dependence of the sensitivity of measurements will then be increased near the surface because of the intermediate bounce. One major problem with this method is the difficulty of obtaining travel-times at the smaller scales as the first-skip waves interfere with the signal from the second skip: we lack data for the shallowly penetrating waves.

We evaluated the effectiveness of these methods with a simple experiment as illustrated in Fig. 2. An artificial signal (panel (a) of Fig. 2) with periodic structure was combined with the forward model to produce travel-times, which were then inverted without the addition of noise, to recover a best-case result. The use of these methods that ignore some of the signal clearly degrades the quality of the solution. This is particularly evident for the shallow layers of the second-skip results were the lack of corresponding data seems to undermine the results.

For the remainder of this work we refer to the uncropped first-skip approach outlined here as the 'standard analysis'.

3. ANALYZING THE SPOT REGION

Two active regions have been studied, each of which contained an isolated spot close to disk centre, crossing the central meridian on April 11$^{\rm th}$ 2002 and April 13$^{\rm th}$ 2002 respectively, see Fig. 1). Note that because the instrument observes a disk centred approximately five degrees below the solar equator, the April 13$^{\rm th}$ spot will suffer from some projection effects in comparison with the April 11$^{\rm th}$ case. This centre-annulus method was repeated with the centre at each pixel of the instrument data, and with several different annular radii, the cross-correlations were then fitted as described in § 2 and the mean phase travel-times recovered.

The April 11$^{\rm th}$ spot was investigated using the standard analysis and also with the different techniques outlined above. The travel times obtained from the GONG dataset were used. Fig. 3 shows horizontal slices through two of the recovered models, for the standard analysis and for a cropped dataset. Using a cropped dataset produces results that agree well with those of the standard analysis, however with the cropped data the results become more horizontally smeared.

In Fig. 4 the standard-analysis and second-skip results are compared. Here the shape of the spot region is not very similar in shape and size except perhaps in the 3.0-6.0 Mm layer. The background pattern also shows a difference between the two methods. We see that the inversion of second-skip data fails to reveal the shallow-layer sign change expected from the standard analysis: this is

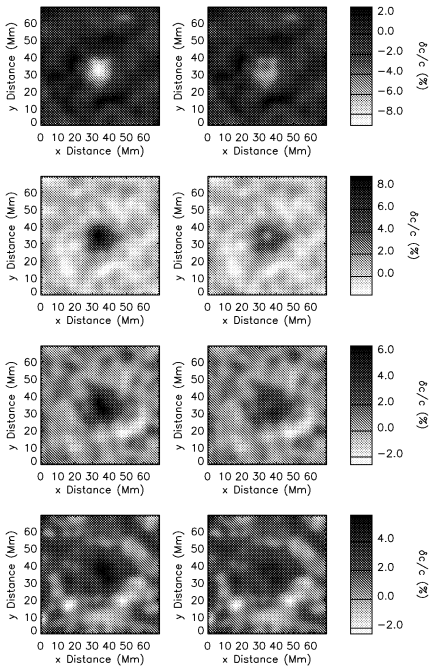

Figure 3. Horizontal slices through the inferred sound-speed perturbations under the April 11$^{\rm th}$ spot, derived from GONG first-skip data. The left column shows results from all the data, the right column the results when data from the spot-region have been cropped.From top to bottom the rows correspond to the depth ranges 1.7 - 2.3 Mm, 3.6 - 4.4 Mm, 6.2 - 7.3 Mm and 8.5 - 9.8 Mm.

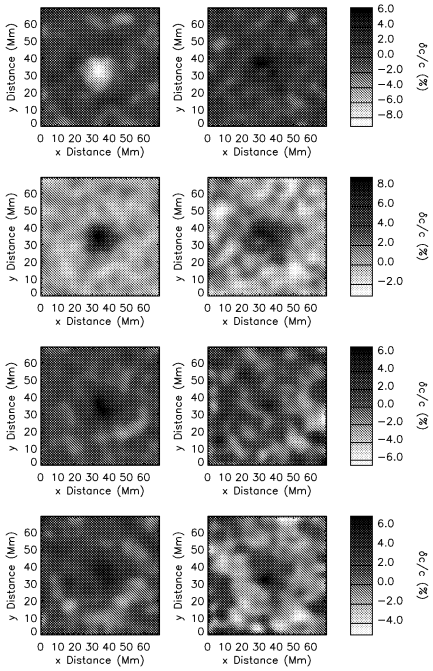

Figure 4. As Fig. 3, but comparing the results from first-skip data (left) and second-skip data (right).

almost certainly due to the lack of data rather than being a refutation of previous inversions, e.g. Kosovichev et al. (2000). The problem seen in the synthetic experiments with the overlap of the first- and second-skip packets for small annular radii is probably to blame.

Analysis was then carried out for the two different spot regions with the data from both instruments. The sound-speed results are shown in Fig. 5 for the April 11$^{\rm th}$ spot. Here we see a similar dependence in depth of the perturbation including a change of sign above about 4 Mm. The horizontal structures of the two solutions are of similar size, shape and distribution, but the region attributable to the spot itself compares less well below 6 Mm. Note the bipolar region that appears in the top-right panel of the figure but is not evident in the GONG results i.e. the top left-hand panel.

The set of horizontal slices in Fig. 6 for the April 13$^{\rm th}$ spot reveals that the general structure of the sound-speed anomalies is similar to the results from April 11$^{\rm th}$. The magnitude of the sound-speed perturbation is slightly weaker than in the previous case and the negative shift in the shallow layers of the GONG results is barely discernible, nevertheless the comparison between the two instruments is perceptibly improved versus the April 11$^{\rm th}$, particularly in the deeper layers where the noise of the two instruments is at a similar level (Rajaguru et al., 2004).

One possible reason for the improved comparison found between the instruments is the observational time periods under analysis. Data gaps in the MDI coverage mean that whilst the selected April 11$^{\rm th}$ GONG data set begins at 01.56 UT, the one for MDI starts later, at 08.00 UT. The April 13$^{\rm th}$ datasets are contemporaneous. The spot may not evolve significantly within a few hours, but the particular realization of the wavefield certainly changes. We suggest that the fact we have the same stochastic noise from the wavefield is primarily responsible for the better agreement between small features in the GONG and MDI inversion results for April 13$^{\rm th}$ compared with April 11$^{\rm th}$. A corollary of this is that these small-scale features are noise, but of solar origin.

We find the maps such as for April 13$^{\rm th}$, which lie further from disk centre, have a gradient across the mean travel-time. This is a consequence of lack of deprojection in our measurements: a given separation in pixels corresponds to a larger physical distance on the solar surface. This can increase the effective travel-time and will also worsen the spatial resolution of the data. These problems degrade the inversion solution for both instruments on April 13$^{\rm th}$. They may also be responsible for the poor recovery of the shallow-layer sign change in the GONG maps (see top-left panel of Fig. 6).

4. DISCUSSION

These inferred structures remain even when the potentially contaminated measurements from inside the spot are excluded, though our horizontal resolution is degraded and the amplitude of the inferred perturbations

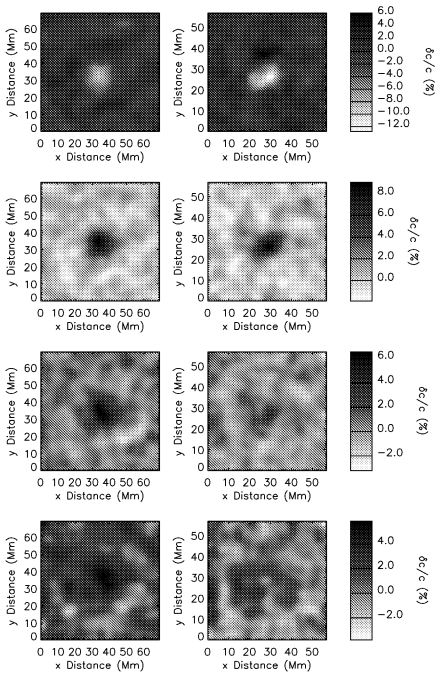

Figure 5. Horizontal slices through the inferred sound-speed perturbations under the April 11$^{\rm th}$ spot, comparing results from GONG data (left) and MDI data (right). The depth ranges in each row are the same as in Fig. 3.

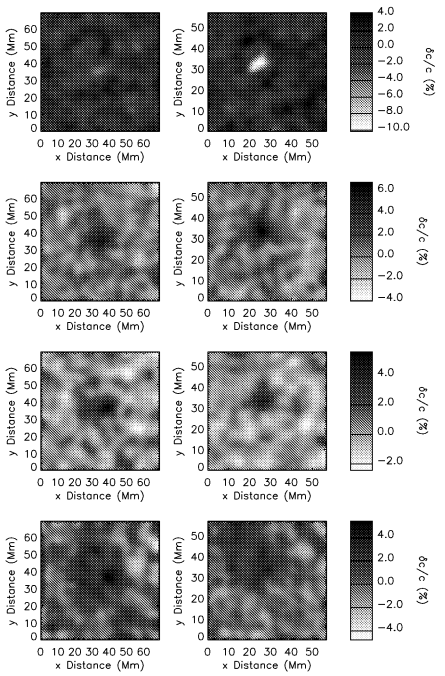

Figure 6. As Fig. 5, but for the spot region of April 13$^{\rm th}$.

is reduced somewhat. We conclude that the apparent change of sign in the sound-speed anomaly beneath sunspots is not purely an artefact caused by using Doppler measurements from within strongly magnetic regions, though those may partly exaggerate the strength of the anomaly.

The good qualitative agreement between the results for the two sunspots suggests that the sign-reversing structure may be generic for isolated and fairly small sunspots such as the pair we have studied.

The GONG data produce results very similar to those of the whole-disk MDI data at depths of about 5 Mm and greater although this is not the case when the observation periods are not the same. This is excellent for potential long-term monitoring of solar sub-surface weather from the GONG network. The slightly lower GONG resolution and the effects of atmospheric seeing on measurements of waves with large horizontal wavenumber put more noise into the GONG travel times for small distances (Rajaguru et al., 2004): for this reason the MDI results are superior in the shallowest layers (see top rows of Figs 5 and 6).

ACKNOWLEDGEMENTS

This work utilizes data from GONG and MDI on the SOHO. The GONG project is supported by the NSF and is carried out by the National Solar Observatory, Tucson, Arizona under AURA. The MDI project is supported by NASA grant NAG5-8878 to Stanford University. SOHO is a project of international cooperation between ESA and NASA. SJH is supported by a studentship from PPARC in the UK and by travel grants from NASA and the CR Barber Trust Fund Institute of Physics. This work supported by PPARC grant no. PPA/G/S/2000/00502.

REFERENCES

Braun, D.C., Time-Distance Sunspot Seismology with GONG Data, *ApJ*, 487, 447 – 456, 1997

Duvall Jr, T.L., Jefferies, S.M., Harvey, J.W. and Pomerantz, M.A., Time-distance helioseismology, *Nature*, 362, 430 – 432, 1993

Duvall Jr, T.L., Time-Distance Helioseismology: an Update, *Proc. GONG 1994. Helio- and Asteroseismology*, ed R.K. Ulrich, E.J. Rhodes Jr and W. Däppen, ASP Conference Series, 76, 465 – 474, 1995

Giles, P., *Time-distance measurements of large-scale flows in the solar convection zone*, PhD Thesis, Stanford University, 2000

Kosovichev, A.G., Duvall Jr., T.L. and Scherrer, P.H., Time-Distance Inversion Methods and Results, *Sol. Phys.*, 192, 159 – 176, 2000

Paige, C.C. and Saunders, M.A., LSQR An algorithm for sparse linear equations and sparse least squares, *ACM Trans. Math. Soft.*, 8, 1, 43 – 71, 1982

Rajaguru, S.P., Hughes, S.J. and Thompson, M.J., Comparison of Noise Properties of GONG and MDI Time-Distance Helioseismic Data, *Sol. Phys.*, 220, 381 – 398, 2004

Zhao, J. and Kosovichev, A.G., Helioseismic Observation of the Structure and Dynamics of a Rotating Sunspot Beneath the Solar Surface, *ApJ*, 591, 446 – 453, 2003